Supplementary information

for

"Electron transfer properties of mono- and diferrocenyl based Cu Complexes attached as self-assembled monolayers on gold electrodes by "self-induced" electroclick"

Christophe Orain[a], Pascal Le Poul[b], Yves Le Mest[a], Nicolas Le Poul[a,*]

[a] *Chimie, Electrochimie Moléculaires et Chimie Analytique, UMR 6521 CNRS, Université de Bretagne Occidentale, 6 Avenue Le Gorgeu 29238 Brest Cedex 03, France*
[b] *Organométalliques et Matériaux Moléculaires,UMR 6226 CNRS, Institut des Sciences Chimiques de Rennes, IUT BP 30219, 22302 Lannion Cedex, France*

Contents

1 Synthesis and characterization of the ligands **3**
1.1 Synthesis and characterization of the ligands **3'** and **4'** 3
1.2 Synthesis and characterization of the ligands **3** and **4** 4
1.3 Synthesis and characterization of compounds **6** and **7** 5

2 UV-Vis and EPR characterizations of Cu-2 and Cu-3 **5**

3 Voltammetric characterization of the Cu complexes in acetonitrile **5**

4 Voltammetric characterization of the immobilized Cu complexes in water **6**

*corresponding author. tel.: +33 2 98 01 61 68
Email address: nicolas.lepoul@univ-brest.fr (Nicolas Le Poul)

5 Calculation of the experimental surface coverage values for the Cu(1-4) complexes by CV peak integration 6

6 Calculation of the theoretical surface coverage values for the Cu(1-4) complexes 6

7 Figures 8

1. Synthesis and characterization of the ligands

*1.1. Synthesis and characterization of the ligands **3'** and **4'***

The general procedure for the pre-functionalization click reaction is as following: the 6-TIPSe-BMPPA (40 mg) and the azide derivative were dissolved in dichloromethane (15 mL) with a 1:1 molar ratio. Two aqueous solutions (7.5 mL each) containing $CuSO_4$, 5 H_2O (0.1 molar equivalent, 2.5 mg) and sodium ascorbate (0.2 molar equivalent, 3.9 mg) were prepared separately. The three solutions were mixed in a flask and stirred vigorously for 48 hours under inert atmosphere at room temperature. Dichloromethane and water (50 mL of each) were then added to the mixture. The aqueous phase was extracted with CH_2Cl_2 (2 × 50mL). Organic phases were collected, washed with water (3 × 75 mL), dried over $MgSO_4$ and filtered over cotton. The solvent was removed with a rotary evaporator.

*1.1.1. Characterization of the ligand **3'** (FcHexTrz-6TIPSeBMPA)*

^{1}H NMR (400 MHz, $CDCl_3$) δ (ppm): 8.54 (1H, d, J = 4Hz, H_a), 7.66-7.53 (5H, m, H_{Py} H_{Trz}), 7.33 (1H, m, H_g), 7.14 (1H, m, H_bH), 4.31 (2H, t, J = 8Hz, TrzCH_2CH2), 4.05 (5H, s, non substituted Cp), 4.01 (4H, s, substituted Cp), 3.86 (2H, s, NCH_2Trz), 3.83 (2H, s, NCH_2Py), 3.81 (2H, s, NCH_2Py), 2.29 (2H, t, J = 8Hz, CH_2Fc), 1.88 (2H, m, H_h), 1.47 (2H, m, H_k), 1.33 (4H, m, H_i H_j), 1.14 (21H, m, Si(iPr)$_3$).

$C_{37}H_{46}FeN_6Si$; MW = 658.73 g.mol^{-1}

*1.1.2. Characterization of the ligand **4'** (BisFcTrz-6eBMPA)*

Compound **4'** was purified by using column chromatography on silica gel with a CH_2Cl_2/MeOH mixture as eluent (methanol ratio from 0 to 5% in volume). The red product was obtained with a 82% yield. ^{1}H NMR (400 MHz, $CDCl_3$) δ (ppm) (E-type isomer): 8.50 (1H, d, J = 4Hz, H_a), 7.62-7.51 (5H, m, H_{Trz} H_{Py}), 7.32 (1H, m, H_g), 7.12 (1H, m, H_b), 6.46 (1H, d, J = 16Hz, HC=CH), 6.35 (1H, d, J = 16Hz, HC=CH), 5.21(2H, s, TrzCH_2Fc), 4.38 (4H, m, H_j H_o), 4.24 (4H, m, H_k H_p), 4.20 (2H, m, H_h), 4.15 (2H, m, H_i), 4.09 (5H, s, non substituted Cp), 3.81 (6H, m, NCH_2), 1.14 (21H, m, Si(iPr)$_3$).

$C_{49}H_{56}Fe_2N_6Si$; MW = 712.44 g.mol^{-1}; yield : 82 %; E/Z mixture (9/1)

*1.2. Synthesis and characterization of the ligands **3** and **4***

The general procedure to remove the TIPS protective group is as following: the compound was dissolved in THF (20 mL). NBu_4F (3 molar equivalents) was then added to the solution. The reaction mixture was stirred for 15 hours. THF was removed with a rotary evaporator.

*1.2.1. Purification and characterization of the ligand **3** (FcHexTrz-6eBMPA)*

Compound **3** was purified by using column chromatography on silica gel with a CH_2Cl_2/MeOH solvent mixture as eluent (methanol ratio from 0 to 3% in volume). ^{1}H NMR (500 MHz, $CDCl_3$) δ (ppm): 8.54 (1H, d, J = 4Hz, H_a), 7.66 7.61 (4H, m, H_{Py}Py H_{Trz}), 7.56 (1H, d, J = 8Hz, H_d), 7.34 (1H, t, J = 4.3Hz, H_g), 7.15 (1H, m, H_b), 4.31 (2H, t, J = 7.3Hz, TrzCH_2CH$_2$), 4.07 (5H, s, non substituted Cp), 4.02 (4H, s, substituted Cp), 3.89 (2H, s, NCH_2Trz), 3.86 (4H, s, NCH_2Py), 3.13 (1H, s, C≡CH), 2.30 (2H, t, J = 7.5Hz, CH_2Fc), 1.88 (2H, m, H_h), 1.47 (2H, m, H_k), 1.33 (4H, m, H_i H_j). ^{13}C NMR (500 MHz, $CDCl_3$) δ (ppm): 159.8, 158.8, 149.4, 143.7, 141.4, 136.7, 130.9, 128.8, 125.9, 123.5, 123.3, 123.1, 122.2, 89.1, 82.9, 68.5, 68.1, 67.1, 59.4, 48.7, 31.0, 30.3, 29.5, 28.9, 26.4. Single Mass Analysis (TOF MS ES+) (MeOH): m/z found: 573.2423 (m/z calculated for $C_{33}H_{37}FeN_6$ $[M+H]^+$: 573.2424).

$C_{33}H_{36}FeN_6$; MW = 572.52 g.mol^{-1}; yield : 44 %

*1.2.2. Purification and characterization of the ligand **4** (BisFcTrz-6eBMPA)*

Compound was purified by using column chromatography on silica gel with a CH_2Cl_2/MeOH solvent mixture as eluent (methanol ratio from 0 to 3% in volume). ^{1}H NMR (500 MHz, $CDCl_3$) δ (ppm) (E-type isomer): 8.50 (1H, d, J = 4Hz, H_a), 7.62-7.58 (3H, m, H_{Trz} H_c H_f), 7.52-750 (2H, m, H_d H_e), 7.32 (1H, d, J = 6.5Hz, H_g), 7.13 (1H, m, H_b), 6.46 (1H, d, J = 16Hz, HC=CH), 6.35 (1H, d, J = 16Hz, HC=CH), 5.22 (2H, s, TrzCH_2Fc), 4.39 (4H, m, H_j H_o), 4.24 (4H, m, H_k H_p), 4.21 (2H, m, H_h), 4.15 (2H, m, H_i), 4.09 (5H, s, non substituted Cp), 3.81 (6H, s, NCH_2), 3.12 (1H, s, C≡CH). ^{13}C NMR (500 MHz, $CDCl_3$) δ (ppm) (E-type isomer): 160.2, 159.1, 149.1, 144.2, 141.3, 136.7, 136.5, 125.8, 125.2, 123.3, 123.1, 122.4, 122.0, 85.3, 83.9, 83.0, 81.3, 70.3, 70.1, 69.9, 69.2, 68.8, 67.0, 66.4, 59.7, 59.5, 49.8, 48.8. Single Mass Analysis (TOF MS ES+) (MeOH): m/z found: 713.1758 (m/z calculated for $C_{40}H_{37}Fe_2N_6$ $[M+H]^+$: 713.1774).

$C_{40}H_{36}Fe_2N_6$; M = 712.44 g.mol^{-1}; yield : 84%; E/Z isomers mixture (9/1)

*1.3. Synthesis and characterization of compounds **6** and **7***

*1.3.1. Synthesis and characterization of compound **6** (BisFcMeOH)*

Bisferrocenecarboxaldehyde **5** (0.47 mmol, 200 mg) was dissolved in a 20 mL mixture of THF and methanol (1:2 v/v). Sodium borohydride ($NaBH_4$) was added slowly and the mixture was kept under stirring at room temperature during 1 hour. The product was extracted with diethyl ether and recrystallized from pentane. The red solid was obtained with a 74 % yield. ^{1}H NMR (400 MHz, $CDCl_3$) δ (ppm): 6.38 (1H, d, J = 12Hz, HC=CH), 6.30 (1H, d, J = 12Hz, HC=CH), 4.43 (4H, m), 4.30 (6H, m), 4.21 (2H, m), 4.17 (5H, s, unsubstituted Cp), 4.10 (2H, s, CH_2OH).

*1.3.2. Synthesis and characterization of compound **7** (BisFcMeN_3)*

Bisferrocenemethanol **6** (0.28 mmol, 120 mg) and sodium azide (6 mol equiv, 110 mg) were dissolved in a 6 mL glacial acid acetic solution, under N_2 atmosphere. The mixture vas heated to 80 °C and stirred for 3 hours. CH_2Cl_2 (100mL) was then added, washed with saturated $NaHCO_3$ solution (3 x 100 mL) and water (1 × 100 mL). The organic layer was dried on $MgSO_4$ and filtered over a hydrophilic cotton. The solvent was removed with a rotary evaporator. The final product was obtained as red solid with a 92 % yield. ^{1}H NMR (500 MHz, $CDCl_3$) δ (ppm): 6.24 (1H, d, J = 12Hz, HC=CH), 5.98 (1H, d, J = 12Hz, HC=CH), 4.68 (2H, m), 4.52 (2H, m), 4.39 (2H, m), 4.24 (6H, m), 4.19 (5H, s, non substituted Cp), 4.03 (2H, s, CH_2N_3).

2. UV-Vis and EPR characterizations of Cu-2 and Cu-3

The spectroscopic signatures of Cu(**1**-**4**) complexes were obtained in CH_3CN. For each measurement, the concentration in Cu complexes was 10^{-3} Mol L^{-1}. EPR spectra have been obtained at T = 150 K. UV-Vis experiments were performed at room temperature.

Related figures: Figure S2; Figure S3; Figure S4; Figure S5; Figure S6.

3. Voltammetric characterization of the Cu complexes in acetonitrile

Cyclic voltammograms of Cu(**1**-**4**) were performed at different scan rates in CH_3CN/KPF_6 with a Pt working electrode. All potential have been recalibrated vs $E^0(Fc^+/Fc)$.

Related figures: Figure S7; Figure S8; Figure S9; Figure S10.

4. Voltammetric characterization of the immobilized Cu complexes in water

Cyclic voltammograms of immobilized Cu(**1-4**) have been performed at different scan rates in a 0.05 M sodium acetate buffer solution (pH=4.5) with $NaBF_4$ as electrolyte (0.05 M). All potential have been measured vs SCE.

Related figures: Figure S11; Figure S12; Figure S13; Figure S14.

5. Calculation of the experimental surface coverage values for the Cu(1-4) complexes by CV peak integration

For all complexes, the surface coverage was determined by integration of the i vs E plots obtained by cyclic voltammetry after correction of the baseline. A Gaussian model was used to fit each peak of the experimental data. The process was operated by using the OriginPro 8 software©. For the Cu-**3** and Cu-**4** complexes, the microscopic systems (Cu and Fc) were deconvoluted. As shown in Figure S15 and Figure S16, good fits were obtained by using this method for both complexes.

Related figures: Figure S15; Figure S16.

6. Calculation of the theoretical surface coverage values for the Cu(1-4) complexes

The compacity C is defined as the maximum surface coverage of immobilized species by unit surface area, according to equation (S.1):

$$C = \frac{4nS_c}{\pi D^2} \tag{S.1}$$

[D is the electrode diameter, n the number of molecules immobilized, S_c is the surface occupied by one species.]

The surface coverage Γ is defined as the number of immobilized species by unit surface:

$$\Gamma = \frac{4n}{N_A\,(\pi D^2)} \tag{S.2}$$

The combination of equations (S.1) and (S.2) yields an expression of the surface coverage as a function of compacity:

$$\Gamma = \frac{C}{N_A S_c} \tag{S.3}$$

Complexes can be assumed as ellipsoidic objects which are organized according to a face-centered cubic (3 dimensional) stacking, with $C = 0.735$ [1]. The surface occupied on the electrode by one ellipsoid can be determined by the calculation of the area of the ellipse,

$$S_c = \pi \times a \times b \tag{S.4}$$

[a is half the length of the small axis of the ellipsoid, b is half the length of the big axis.]

For the ethynylferrocene, the terminal redox center can be considered as a sphere of 3.3 Å radius ($a = b$) [1]. For the Cu complexes, the small axis length ($2 \times a$) has a constant value and is estimated to be 9 Å (diameter of Cu(II)-TMPA assumed as a sphere). The big axis length is obtained by adding the different elements constituting the complex, i.e. the TMPA core, the ferrocenyl group and the spacer. The b values have been estimated by using the Chem3D software©. Values of a, b and Γ_{theo} (mol cm^{-2}) for each complex are gathered in Table S1, according to the equation below:

$$\Gamma_{\text{theo}} = \frac{3.86 \times 10^{-25}}{a \times b} \tag{S.5}$$

Table S1: Theoretical surface coverage (Γ_{theo}) values calculated from estimated a and b

Complex	a / Å	b / Å	Γ_{theo}
$[Cu^{II}\mathbf{1}(L)_n]^{2+}$	4.5	4.5	190
$[Cu^{II}\mathbf{2}(L)_n]^{2+}$	4.5	7.8	110
$[Cu^{II}\mathbf{3}(L)_n]^{2+}$	4.5	10.9	80
$[Cu^{II}\mathbf{4}(L)_n]^{2+}$	4.5	11	80
$[Cu^{II}(6eTMPA)(L)_n]^{2+}$	4.5	4.5	190
eFc	3.3	3.3	360

References: [1] C. E. D. Chidsey, C. R. Bertozzi, T. M. Putvinski, A. M. Mujsce, J. Am. Chem. Soc. 112 (1990) 4301-4306; [2] A. Donev, I. Cisse, D.

Sachs, E. Variano, F. H. Stillinger, R. Connelly, S. Torquato, P. M. Chaikin, Science 303 (2004) 990-993.

7. Figures

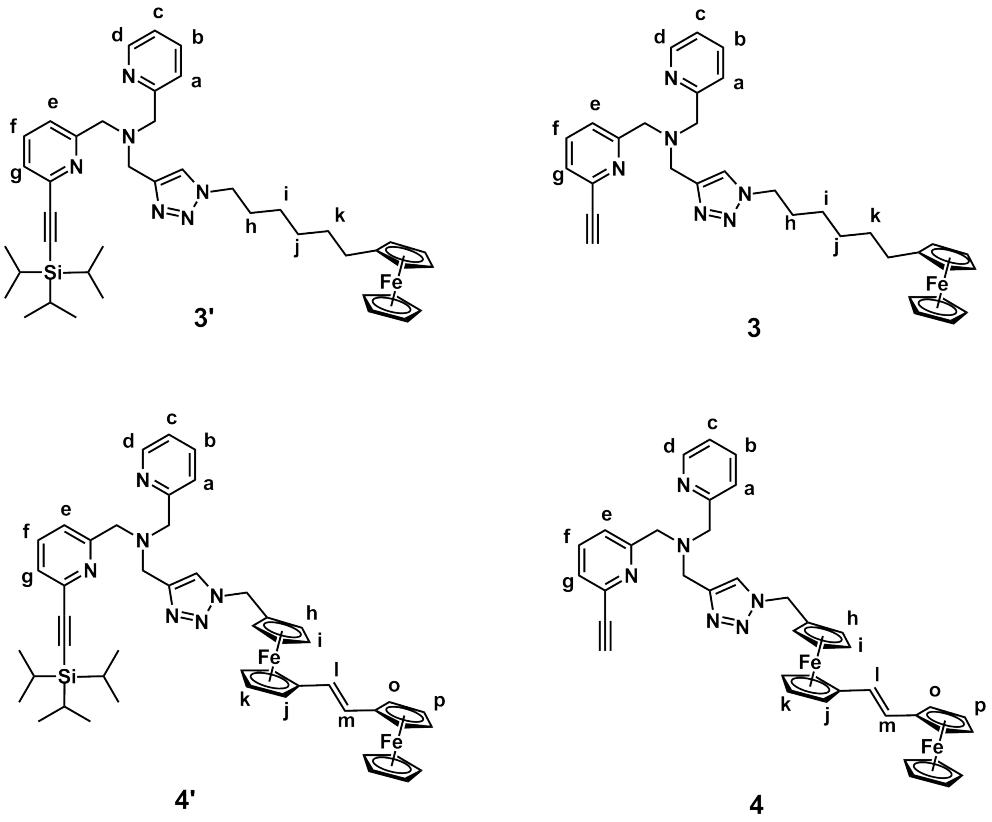

Figure S1: Schematic representation of compounds **3**, **3'**, **4**, and **4'** with indexation for NMR spectrocopy analysis.

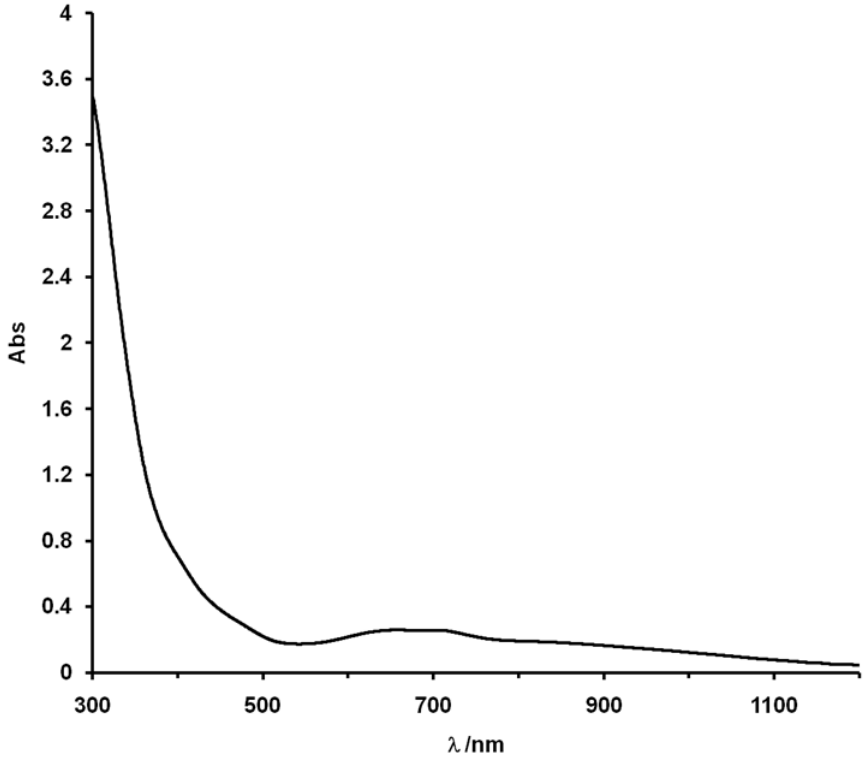

Figure S2: UV-Vis spectrum of Cu-**2** (1 mM) in MeCN

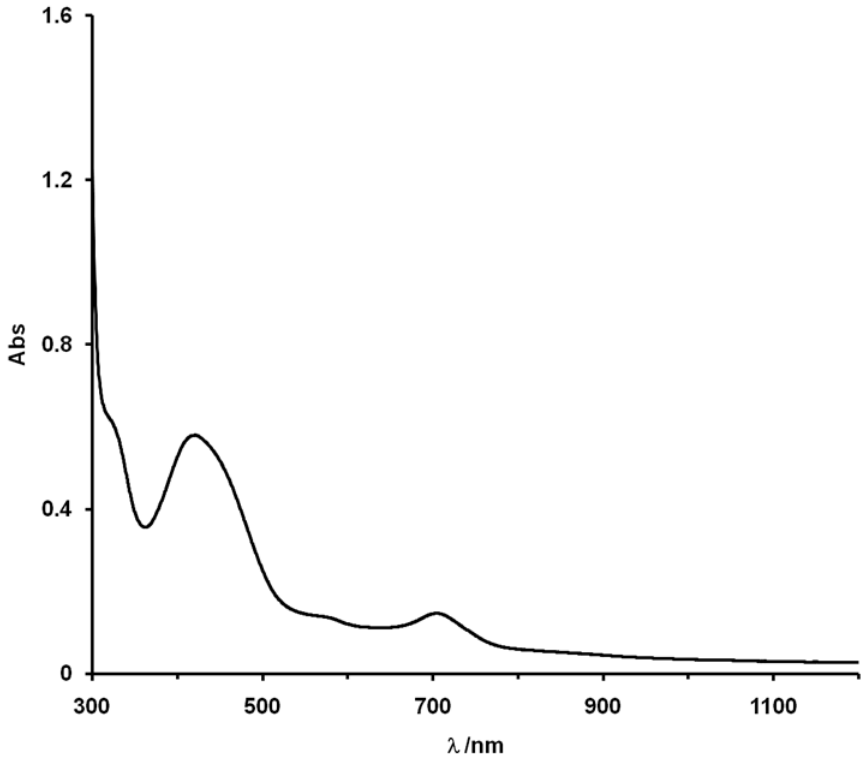

Figure S3: UV-Vis spectrum of Cu-**3** (1 mM) in MeCN

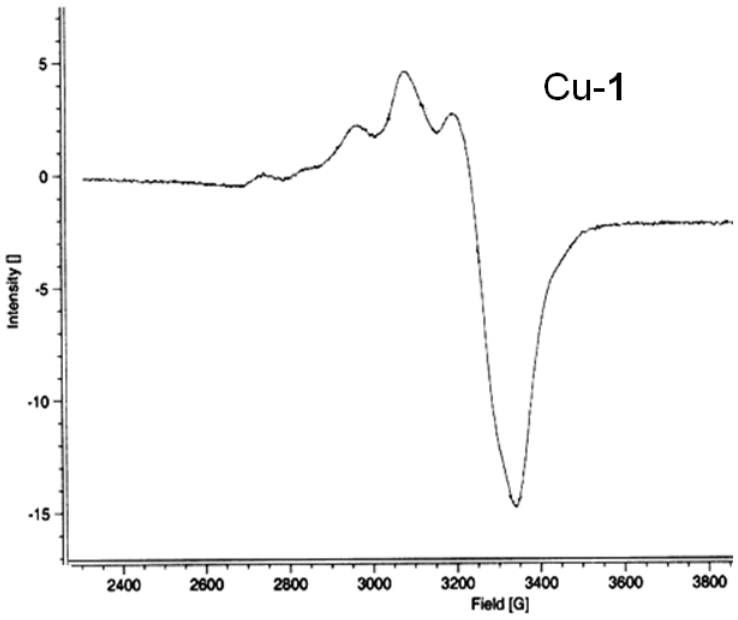

Figure S4: EPR spectrum of Cu-**1** (1 mM) in MeCN at 150 K

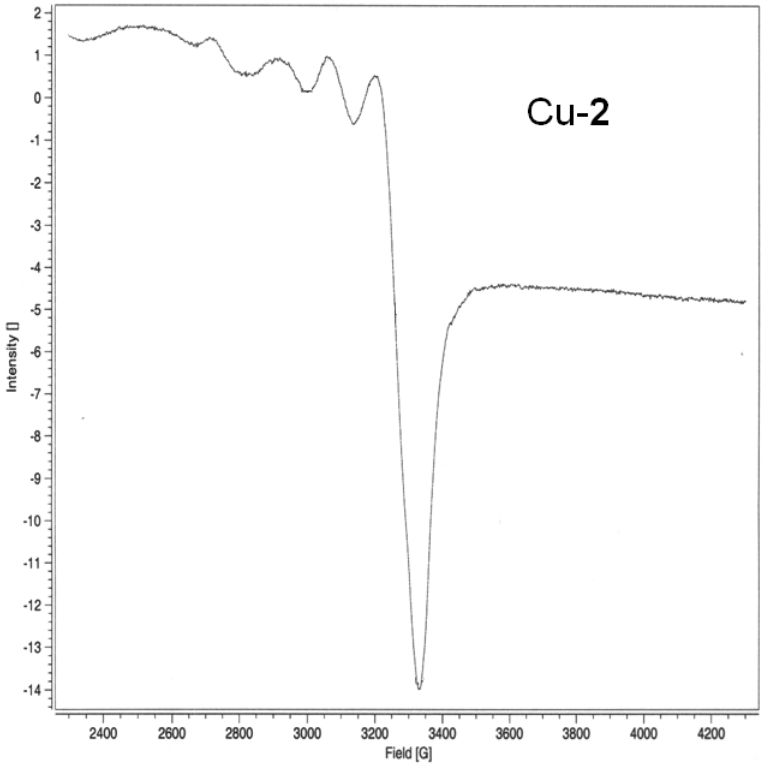

Figure S5: EPR spectrum of Cu-**2** (1 mM) in MeCN at 150 K

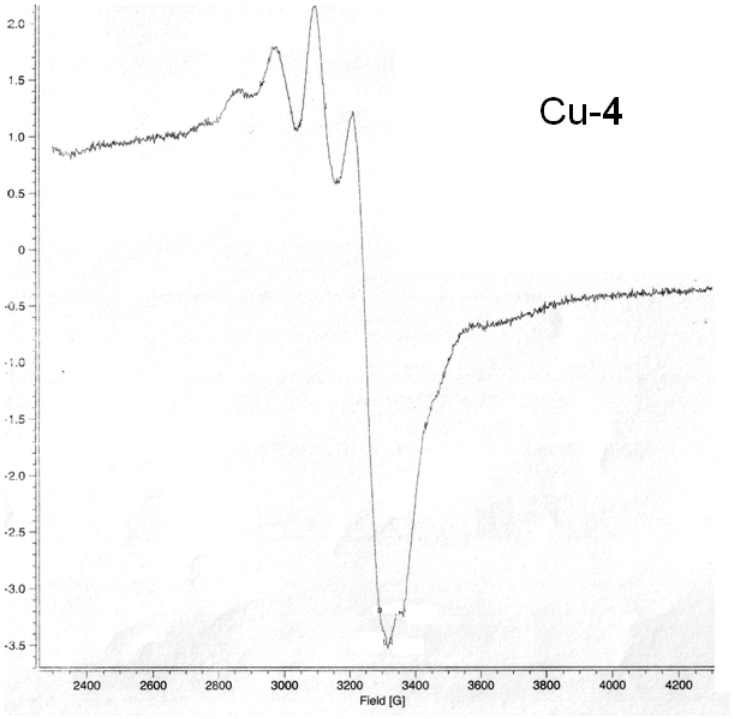

Figure S6: EPR spectrum of Cu-**4** (1 mM) in MeCN at 150 K

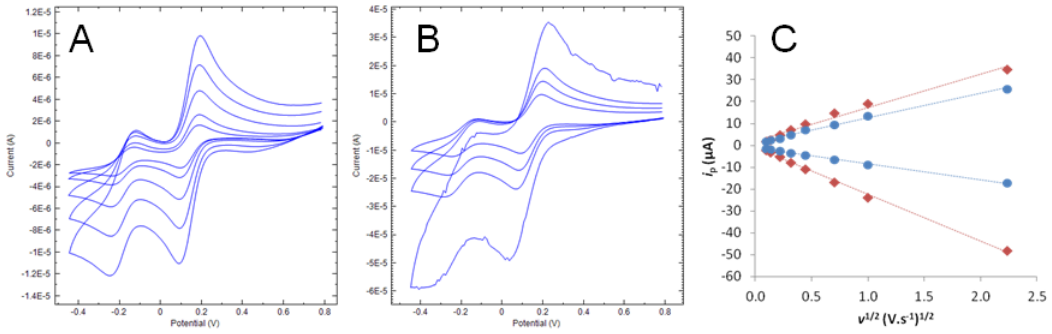

.

Figure S7: CVs at a Pt electrode of Cu-**1** (E vs Fc) in CH_3CN/KPF_6 for A) 0,01 V s $^{-1}$ < v < 0,2 V s $^{-1}$, B) 0,2 V s $^{-1}$ < v < 2 V s $^{-1}$; C) Plots of i_p vs $v^{1/2}$

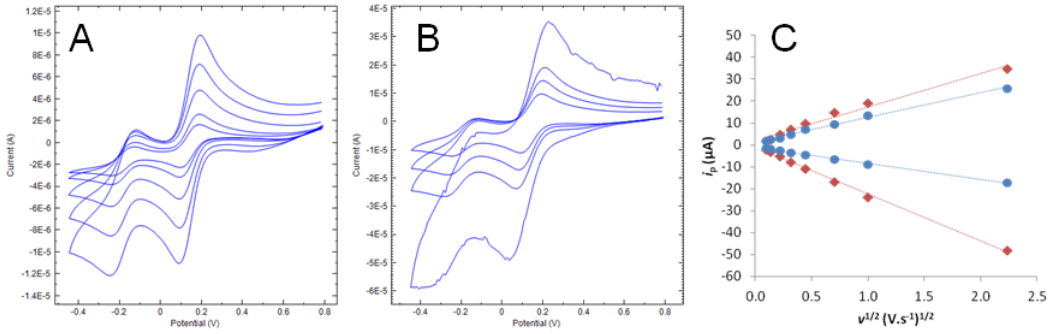

.

Figure S8: CVs at a Pt electrode of Cu-**2** (E vs Fc) in CH_3CN/KPF_6 for A) 0,01 V s $^{-1}$ < v < 0,2 V s $^{-1}$, B) 0,2 V s $^{-1}$ < v < 5 V s $^{-1}$; C) Plots of i_p vs $v^{1/2}$ (Blue: Cu, Red: Fc)

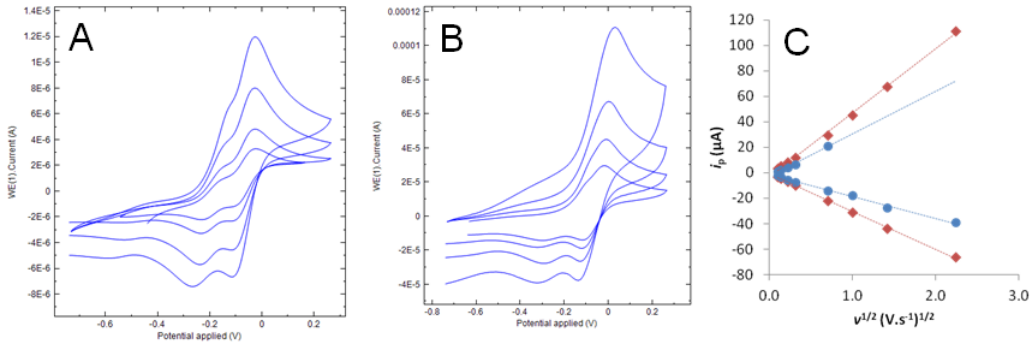

.

Figure S9: CVs at a Pt electrode of Cu-**3** (E vs Fc) in CH_3CN/KPF_6 for A) 0,01 V s $^{-1}$ < v < 0,2 V s $^{-1}$, B) 0,2 V s $^{-1}$ < v < 0.5 V s $^{-1}$; C) Plots of i_p vs $v^{1/2}$(Blue: Cu, Red: Fc)

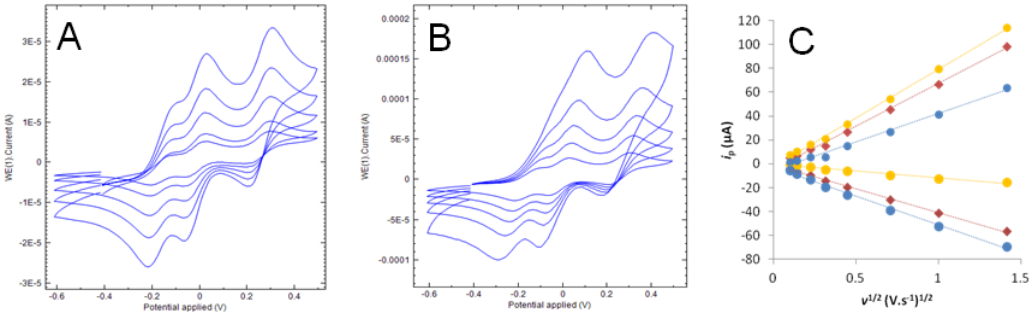

.

Figure S10: CVs at a Pt electrode of Cu-**4** (E vs Fc) in CH_3CN/KPF_6 for A) 0,01 V s $^{-1}$ < v < 0,2 V s $^{-1}$, B) 0,2 V s $^{-1}$ < v < 5 V s $^{-1}$; C) Plots of i_p vs $v^{1/2}$(Blue: Cu, Red: monosubstituted Fc, Yellow; disubstituted Fc)

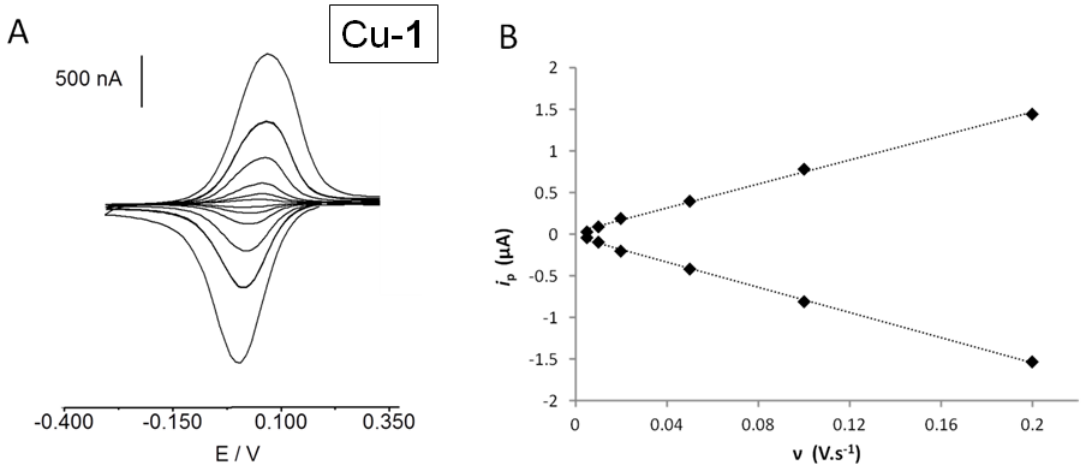

.

Figure S11: A) CVs in $H_2O/NaBF_4$ for 0,005 V s $^{-1}$ $< v <$ 0,2 V s $^{-1}$ of Cu-**1** immobilised on gold (E vs SCE). B) Plots of i_p vs v

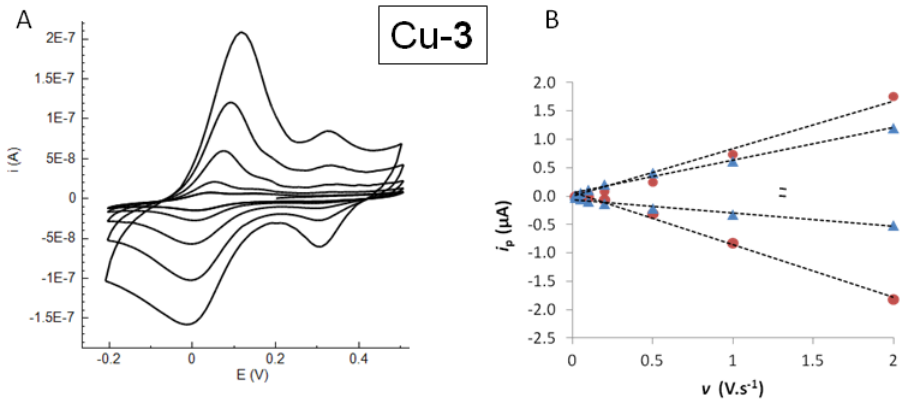

.

Figure S12: A) CVs in $H_2O/NaBF_4$ for 0,01 V s $^{-1}$ $< v <$ 0,2 V s $^{-1}$ of Cu-**3** immobilised on gold (E vs SCE). B) Plots of i_p vs v

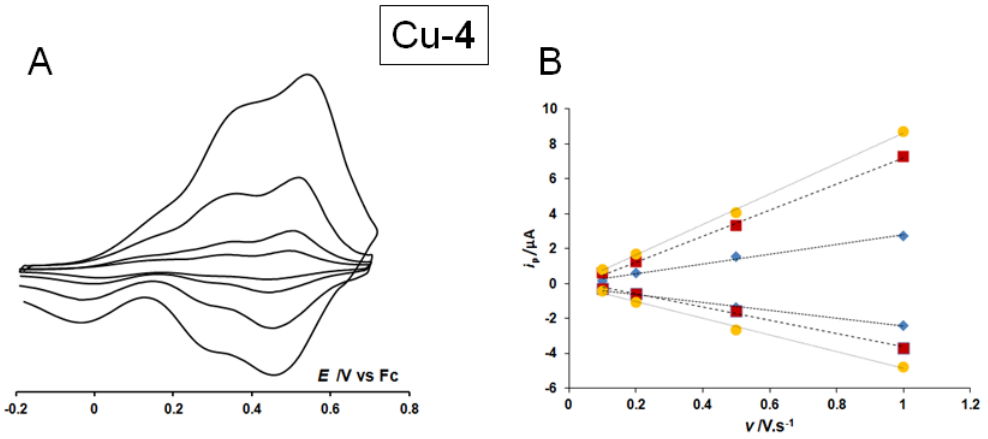

.

Figure S13: A) CVs in $H_2O/NaBF_4$ for 0,1 V s $^{-1}$ $< v <$ 1 V s $^{-1}$ of Cu-**4** immobilized on gold (E vs SCE). B) Plots of i_p vs v

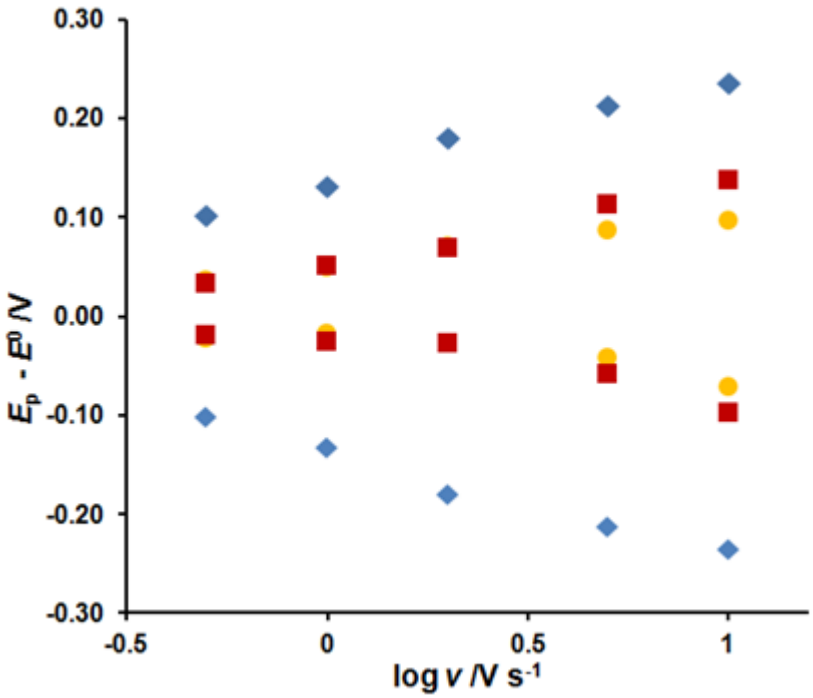

.

Figure S14: Plots of E_p vs log (v) (Blue: Cu, Red: mono-substituted Fc, Yellow; di-substituted Fc) from CVs in $H_2O/NaBF_4$ for 0,05 V s $^{-1}$ < v < 0,5 V s $^{-1}$ of Cu-**4** immobilized on gold (E_p re-calibrated vs E^0 for each system)

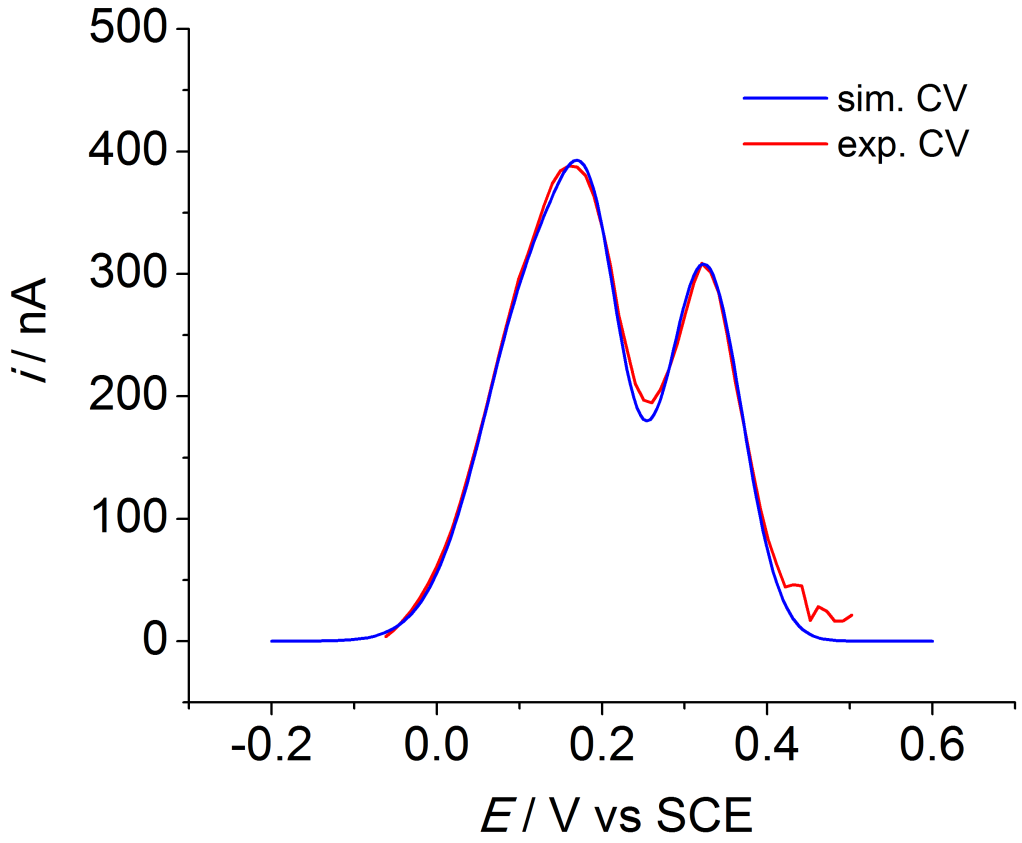

Figure S15: Experimental and simulated CVs (oxidation part) of Cu-**3**. The simulated curve was obtained by generation of Gaussian curves after baseline correction

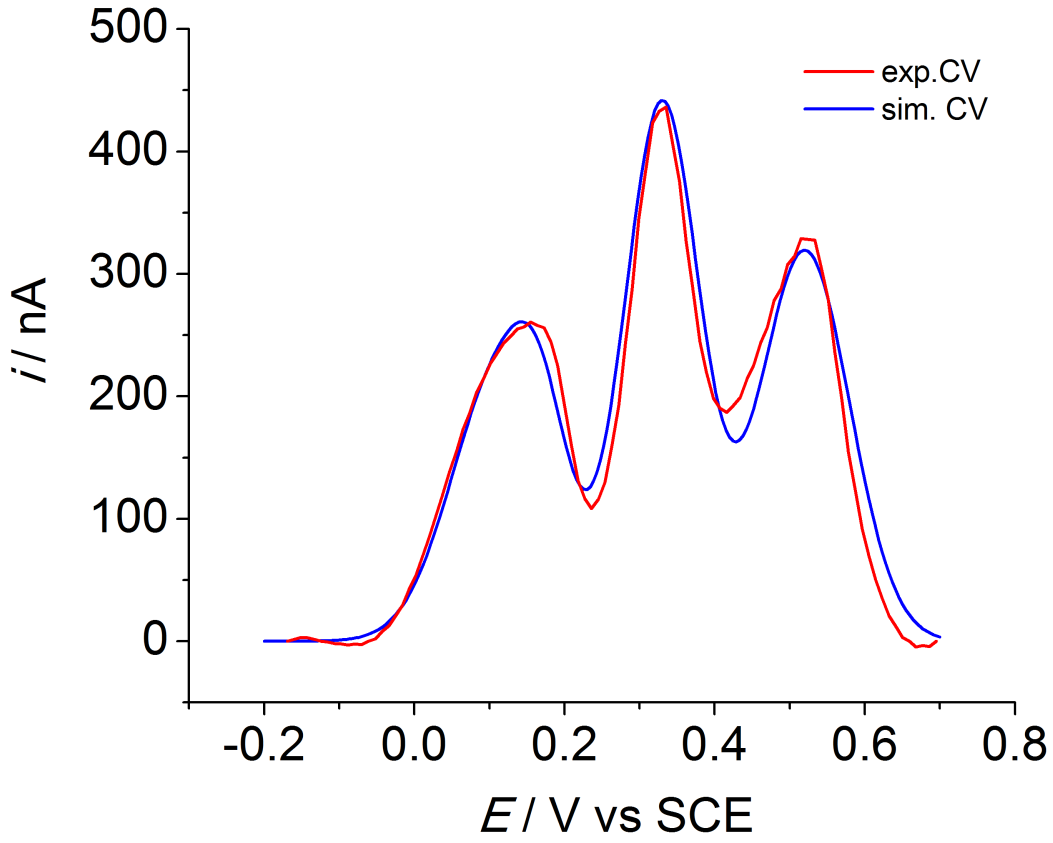

Figure S16: Experimental and simulated CVs (oxidation part) of Cu-**4**. The simulated curve was obtained by generation of the Gaussian curves after baseline correction